

Photon-mediated Peierls Transition of a 1D Gas in a Multimode Optical Cavity

Colin Rylands,¹ Yudan Guo,^{2,3} Benjamin L. Lev,^{2,3,4} Jonathan Keeling,⁵ and Victor Galitski¹

¹*Joint Quantum Institute and Condensed Matter Theory Center,
University of Maryland, College Park, MD 20742, USA*

²*Department of Physics, Stanford University, Stanford, CA 94305, USA*

³*E. L. Ginzton Laboratory, Stanford University, Stanford, CA 94305, USA*

⁴*Department of Applied Physics, Stanford University, Stanford, CA 94305, USA*

⁵*SUPA, School of Physics and Astronomy, University of St Andrews, St Andrews KY16 9SS UK*
(Dated: September 5, 2022)

The Peierls instability toward a charge density wave is a canonical example of phonon-driven strongly correlated physics and is intimately related to topological quantum matter and exotic superconductivity. We propose a method to realize an analogous *photon*-mediated Peierls transition. We consider a system of one-dimensional tubes of interacting Bose or Fermi atoms trapped inside a multimode optical cavity. Pumping the cavity transversely engineers a cavity-mediated metal-to-insulator transition in the atomic system. For the case of strongly interacting bosons in the Tonks-Girardeau limit, this transition can be understood (through fermionization) as being the Peierls instability. We extend our results away from this limit to finite values of the interaction strength as well as to interacting fermions. Both the cavity field and the mass gap display nontrivial power law dependence on the dimensionless matter-light coupling constant.

Introduction — The interaction between electrons and phonons has traditionally played a leading role in the formation of quantum phases of matter, with superconductivity being a prime example. Quantum simulation provides an enticing platform to explore new phases [1], but unfortunately, phonon-driven physics lies beyond traditional optical lattice capabilities as they are externally imposed and rigid. The use of high-finesse optical cavities has been suggested as a route to overcome this by making the optical lattice fully dynamical and compliant [2, 3]. This requires cavities that support multiple degenerate modes, as single-mode cavities only allow dynamics of the lattice intensity, not its period. That is, while single-mode cavities have provided access to a diverse array of exotic quantum phenomena including self-organization [4], supersolids [5], spinor density-wave polariton condensates [6], dynamical Mott insulators [7, 8], and dynamical spin-orbit coupling [9], only multimode cavities support fully emergent optical lattices whose amplitude *and* periodicity may vary [2, 3]. Experiments with multimode cavities have already been used to engineer a variety of interatomic interactions mediated by photons [10–13]. These could subsequently lead to the creation or realization of new many-body systems and states of matter such as quantum liquid crystals made of photons and superfluid atoms [2, 3] and superfluids exhibiting Meissner-like effects [14].

We present how multimode cavities coupled to one dimensional (1D) quantum gases enable the engineering and control of atomic analogues of the interactions between electrons and phonons. Uniquely, 1D ultracold gases allow one to explore pairing physics in bosonic systems, since resonant atomic collisions provide a knob for making bosons strongly repel [15, 16], even to the point that they behave like fermions [17–19]. For such

systems, the addition of *attractive* interactions can result in dramatic effects. Indeed, for 1D systems, even *weakly* attractive interactions result in instabilities leading to strong correlations such that the quasiparticle picture breaks down and collective modes emerge [20–22]. A paradigmatic example is the Peierls instability that occurs because the susceptibility of a free Fermi gas diverges due to infinitesimal density perturbations at twice the Fermi wavevector [23]. If free phonons exist—i.e., if an emergent lattice can match this wavevector—then the result is that the system undergoes a metal-insulator transition via the dynamical generation of a mass gap. The Peierls transition is a canonical example of phonon-driven physics and intimately related to the continuum Su-Schrieffer-Heeger (SSH) model of 1D topological insulators in 1D [24]; Realizing a *photon-mediated* Peierls transition opens new avenues toward exploring the role of Fermi surface nesting and charge density waves in exotic superconductors in simulators operating in a quantum-optical, many-body context.

In this work, we study the existence of such a transition where photons, as mediators of attractive interactions, play the role of phonons. We show that a Peierls instability occurs in a strong, repulsively interacting 1D *bosonic* gas trapped inside a transversely pumped multimode optical cavity. We find that by tuning the interatomic interactions to the hard-core, Tonks-Girardeau (TG) limit [25, 26], the cavity can mediate a Peierls transition in the bosonic gas, with a mass gap and photon amplitude which is exponential in the matter-light coupling. We then extend these calculations to finite values of the interatomic interaction, as well as to interacting fermionic systems. The cavity can mediate a metal-insulator transition, albeit one of different character, in these scenarios as well. For such cases, the

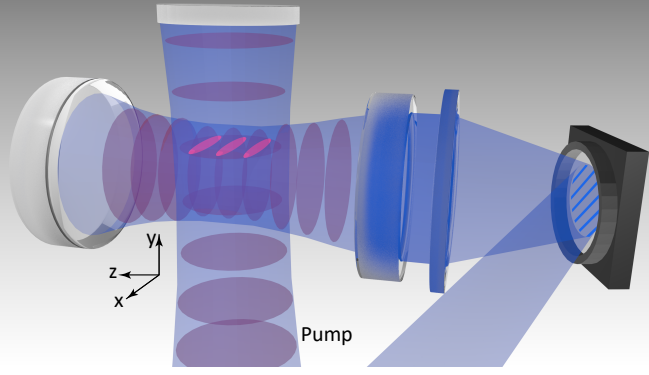


FIG. 1. Schematic of our system. A gas of interacting neutral atoms is placed inside an optical cavity that supports many degenerate spatial modes such as a confocal cavity. A transverse pump (blue) along \hat{y} scatters photons off the atoms (red) into the multimode cavity field (blue). The gas is confined along \hat{x} by a 2D optical lattice (purple) and offset from the center along \hat{y} to avoid mirror-image interactions [11]. The amplitude and phase of the emitted field is imaged via holographic reconstruction of a spatial heterodyne signal formed by interfering part of the pump with the cavity emission.

dynamically generated mass gap and photon amplitude have a nontrivial, power law dependence on the matter-light coupling; this is indicative of the strongly correlated nature of an interacting 1D system. Self-organization of fermions in a single-mode cavity has been previously discussed theoretically [27–29]. That case differs because the diverging susceptibility occurs only when the single cavity mode and Fermi wavevectors are commensurate, and does not permit the self-consistent emergence of the Peierls instability.

Model — Our system, as depicted in Fig. 1, consists of 1D tubes of atoms placed in a transversely pumped multimode optical cavity, such as a confocal cavity [30]. To achieve a 1D trap geometry and uniform atom-cavity coupling, we confine bosonic atoms in a strong λ_T -periodic 2D optical lattice formed by a retroreflected beam along the \hat{y} pump direction and an intracavity standing wave along the \hat{z} cavity axis. The external pump along the \hat{y} has a wavevector k_r close to a degenerate cavity resonance. By choosing the tube-lattice period such that $k_r \lambda_T / 2\pi$ is an integer, the tubes lie at the peaks of the pump and cavity standing-wave fields so the atoms coherently Bragg scatter light into the cavity. As a result, in contrast to experiments on self-organization [31], there is no spontaneous atomic organization in the yz plane; rather, the atoms superradiantly emit into the cavity regardless of pump strength. We choose the tubes to be near the cavity midplane $z = 0$, and the long Rayleigh range of a confocal cavity ensures that the tubes at different z will behave identically. In the x - y plane, all the tubes have the same center location along y . Degenerate confocal cavities with BECs in optical traps are practicable with existing technology [13].

We can write the Hamiltonian of the system as follows; see Supplemental Material for details [32]:

$$H = H_{\text{cav}} + \int dx \sum_{t=1}^{N_z} \left\{ \Psi_t^\dagger(x) \left[-\frac{\hbar^2}{2m} \partial_x^2 - \mu \right] \Psi_t(x) + c \Psi_t^\dagger(x) \Psi_t(x) \Psi_t^\dagger(x) \Psi_t(x) - g \Phi_t(x) \rho_t(x) \right\}. \quad (1)$$

The first term, $H_{\text{cav}} = \hbar \sum_{\alpha,\nu} \omega_{\alpha,\nu} a_{\alpha,\nu}^\dagger a_{\alpha,\nu}$, describes the cavity photons. We sum over different families of nearly degenerate cavity modes labeled by the longitudinal index α and transverse index ν ; the extent of this sum is discussed below. The second and third terms describe the atomic system wherein $\Psi_t(x)$ and $\Psi_t^\dagger(x)$ are the field operators for the bosons which have mass m and chemical potential μ . They interact via a point-like density-density interaction of strength c , and their density operator is given by $\rho_t(x) = \Psi_t^\dagger(x) \Psi_t(x)$. The subscript t labels the tubes, and we take these to be arranged in an array of N_z tubes along \hat{z} [33]. If the tubes are spaced by a multiple of λ_T then the atoms superradiantly scatter the pump into the cavity with intensity $\propto N_z^2$ [34].

The last term describes the coupling of the atomic density to the cavity photons, as induced by the pump. The photon field is written as a sum of the transverse modes of the cavity, $\Phi_t(x) = \sum_{\alpha,\nu} c_\nu^\alpha \tilde{\Xi}_\nu(x) a_{\alpha,\nu}^\dagger + \text{h.c.}$. The transverse mode functions $\tilde{\Xi}_\nu(x)$ are Gauss-Hermite functions of order (l_ν, m_ν) in the x and y directions, respectively, convolved with the Gaussian tube profile in the y direction; see Ref. [32]. We will consider only even families so that the mode index $n_\nu = l_\nu + m_\nu$ is even. As described in Ref. [12], the longitudinal mode function in the cavity gives rise to the factor $c_\nu^\alpha = \cos(\xi^\alpha - \pi n_\nu / 4)$. This includes the effects of the Gouy phase, leading to the n_ν dependence. The choice of which families are included is set by the frequency of the pump; we consider the case where there are two pump frequencies, coupling to two mode families, for which $\xi^\alpha = 0, \pi/2$. This choice ensures that the effective cavity-mediated interaction is local [12]. The prefactor $g = \hbar g_0 \Omega / \Delta_a$ is the effective matter-light coupling where g_0 is the bare coupling, Ω the pump Rabi frequency, and Δ_a is the pump-atom detuning.

Both the matter-light coupling and interatomic interaction strength are experimentally tunable parameters [1]. In particular, the system may be tuned into the TG regime, i.e. $\gamma \equiv mc/\hbar^2 \rho_0 \rightarrow \infty$, using tight trapping and collisional resonances, where ρ_0 is the average 1D density [17, 18]. The atoms behave like free fermions in this limit [25, 26] and so will exhibit a Peierls instability. Even strongly repulsive bosons away from the TG limit exhibit this instability.

Steady state — We investigate the Peierls instability using a mean-field description of the photon field. The

Heisenberg equations for the photon operators are:

$$\dot{a}_{\alpha,\nu}^\dagger = (i\omega_{\alpha,\nu} - \kappa)a_{\alpha,\nu}^\dagger - i\frac{g}{\hbar} \sum_t \int dx c_\nu^\alpha \tilde{\Xi}_\nu(x) \rho_t(x), \quad (2)$$

where we have included a term $\propto \kappa$ accounting for cavity losses. Taking their expectation value and assuming a steady state, the mean field is

$$\langle \Phi_t(x) \rangle = \int dx' \sum_{\alpha,\nu,t'} \frac{2g\omega_{\alpha,\nu}(c_\nu^\alpha)^2}{\hbar(\omega_{\alpha,\nu}^2 + \kappa^2)} \times \tilde{\Xi}_\nu(x) \tilde{\Xi}_\nu(x') \langle \rho_{t'}(x') \rangle. \quad (3)$$

For simplicity, we consider the perfectly degenerate limit $\omega_{\alpha,\nu} = \omega$. Pumping two sequential families of modes (i.e., one free spectral range apart), we have $\sum_\alpha (c_\nu^\alpha)^2 = 1$, allowing the sum over modes to be carried out explicitly [12]: $\sum_\nu \tilde{\Xi}_\nu(x) \tilde{\Xi}_\nu(x') = \frac{w_0^2}{2\sqrt{4\pi\sigma_T}} \delta(x - x')$ [35]. Here, σ_T is the transverse width of an individual tube, and we made a simplifying assumption that the tubes are in the upper half of the cavity, $y > 0$, to avoid mirror-image interactions [11]. Assuming all tubes behave identically, we can insert this into Eq. (3) to give:

$$g \langle \Phi(x) \rangle = \pi \hbar v_F \eta \langle \rho(x) \rangle, \quad \eta \equiv \frac{g^2 N_z \omega w_0^2}{\sqrt{4\pi\sigma_T} \pi \hbar^2 v_F (\omega^2 + \kappa^2)}, \quad (4)$$

where we have defined the dimensionless matter-light coupling η and $v_F = \pi \hbar \rho_0 / m$ is the Fermi velocity in the TG limit. Later, it will be convenient to parameterize this as $\langle \Phi(x) \rangle \equiv \Phi_0(x) + \Phi_{2\pi\rho_0}(x) [e^{2i\pi\rho_0 x} + e^{-2i\pi\rho_0 x}]$ and also introduce the quantity $\Delta \equiv |g\Phi_{2\pi\rho_0}|$. The atoms will coherently scatter light into the cavity, so any nonzero density of atoms implies $\langle \Phi \rangle \neq 0$. Additionally, we will find that $\Phi_{2\pi\rho_0}(x)$ becomes nonzero at the Peierls transition, leading to the dynamical generation of an energy gap in the atomic system.

Adiabatic elimination of photons from the mean-field equations can lead to completely conservative dynamics defined by an effective Hamiltonian [36], and the steady-state condition becomes equivalent to the minimization of the energy of this effective Hamiltonian. The atomic and atom-cavity coupling parts of this effective Hamiltonian come from substituting Eq. (4) into Eq. (1) (considering a single tube), while the cavity part can be written as $H_{\text{cav}}^{\text{eff}} = \frac{g^2}{2\pi \hbar v_F \eta} \int dx \langle \Phi(x) \rangle^2$. We consider only constant values of Φ_0 and $\Phi_{2\pi\rho_0}$, in which case Φ_0 field can be absorbed into a redefinition of the chemical potential, μ . Henceforth we shall deal only with $\Phi_{2\pi\rho_0}$.

Low energy & Bosonization — The atomic system can be described using bosonization, which provides us with a description of our system in terms of two new bosonic fields, $\phi(x)$ and its canonical conjugate $\partial_x \theta(x)$ [20, 21, 37, 38]. The former is related to the atomic density via $\rho(x) = [\rho_0 - \frac{1}{\pi} \partial_x \phi(x)] \sum_{n=-\infty}^{\infty} e^{2in[\pi\rho_0 - \phi(x)]}$, while the

latter is related to the current in the system [38]. In terms of these, the steady-state condition Eq. (4) reduces to $g\Phi_{2\pi\rho_0} = 2\pi \hbar v_F \eta \rho_0 \langle \cos[2\phi(x)] \rangle$. Meanwhile, the effective mean-field Hamiltonian written in terms of the bosonized fields becomes

$$H^{\text{eff}} = H_{\text{cav}}^{\text{eff}} + \frac{\hbar v_F}{2\pi} \int dx \left\{ \frac{1}{K^2} [\partial_x \phi(x)]^2 + [\partial_x \theta(x)]^2 \right\} \pm 2\Delta \int dx \rho_0 \cos[2\phi(x)]. \quad (5)$$

The first line describes the pure atomic and cavity systems. The interatomic interactions are encoded via the newly introduced parameter K which depends on c in a complicated fashion [39]. For large repulsive interactions, this relationship can be approximated by $K \approx 1 + 4\hbar^2 \rho_0 / mc + \mathcal{O}\{(\hbar^2 \rho_0 / mc)^2\}$, with the TG limit achieved at $K = 1$, while $K = \infty$ corresponds to free bosons [39]. The second line describes the matter-light coupling and will generate a gap. We have allowed for the possibility that the matter-light coupling and photon field might carry opposite signs. We keep only terms which are most relevant in a renormalization group sense which restricts our analysis to values $1/2 < K < 2$.

While in the present work our primary system of interest consists of bosons with short-range, repulsive interactions, bosonization allows one to also describe the low-energy physics of bosons with long-range interactions or interacting fermions [20, 21, 40]. Such systems can be described by a Luttinger parameter with $0 < K < 1$, and so in the following, we allow for arbitrary values of $1/2 < K < 2$. Results derived for $K > 1$ are applicable to bosonic systems with short-ranged interactions or fermionic systems with attractive interactions, whereas $K < 1$ corresponds to repulsive fermions or bosonic systems with long-range interactions.

Tonks-Girardeau limit — The atoms behave as free fermions in the TG limit [25, 26]. This is evident in our low-energy description at $K = 1$ where it is possible to express the bosonic operators as a pair of chiral fermions, $\psi_\pm^\dagger(x) = \sqrt{\rho_0} e^{\mp i\phi(x) - i\theta(x)}$. In terms of these, the low-energy Hamiltonian, Eq. (5) becomes the 1D Dirac Hamiltonian [41] and the problem reduces to;

$$[-i\hbar v_F \partial_x - \epsilon_n] u_n(x) = \pm \Delta v_n(x) \quad (6)$$

$$[i\hbar v_F \partial_x - \epsilon_n] v_n(x) = \pm \Delta u_n(x). \quad (7)$$

Here, $u_n(x) = u_n e^{ik_n x}$ and $v_n(x) = v_n e^{ik_n x}$ are the wave functions of the right and left moving fermions, and ϵ_n are the single particle energy levels. The steady-state condition now becomes

$$\Delta = \pi \hbar v_F \eta \sum_n (u_n v_n^* + v_n^* u_n) = -\pi \hbar v_F \eta \frac{d\varepsilon_{\text{gs}}(\Delta)}{d\Delta}, \quad (8)$$

where ε_{gs} is the ground-state energy density of the atomic part of the system, and we hold the chemical potential

fixed so that there are $N = \rho_0 L$ particles. These equations are the same as in the SSH model [24]. Their solution is well known, and carrying it over to the present case, we find that $g\Phi_{2k_F} = \pm 2\pi\hbar v_F \rho_0 e^{-1/\eta}$. The self-consistent photon field is therefore given by

$$\langle \Phi(x) \rangle = \pm \frac{4\pi\hbar v_F}{g} \rho_0 e^{-1/\eta} \cos(2k_F x). \quad (9)$$

In addition, we have that $\epsilon_n(\Delta) = \pm \sqrt{(\hbar v_F k_n)^2 + \Delta^2}$, which shows that the system is insulating with an energy gap of 2Δ . The applicability of the low-energy description relies on the Fermi energy, $E_F = \pi\hbar v_F \rho_0$, being the largest scale in the system. In particular, we require that $\Delta < E_F$, which in turn requires $\eta < 1$.

Finite interaction — The system is quite different for $K \neq 1$. It is strongly correlated and interacting, but can no longer be mapped to the SSH model. Nevertheless, an exact solution for the steady state can be found, although the cases of positive and negative $g\Phi_{2\pi\rho_0}$ need to be treated separately; we will find below that these correspond to $K > 1$ and $K < 1$, respectively. For $g\Phi_{2\pi\rho_0} < 0$, the atomic part of the Hamiltonian is that of the Sine-Gordon or massive Thirring model with a positive mass term [20, 21, 37]. This is an exactly solvable field theory and many of its properties are well known [42, 43]. In particular, the mass gap of the model becomes renormalized due to the interactions,

$$\frac{\Delta_R^+}{\pi\hbar v_F \rho_0} = \xi_+ \left[\frac{\Delta}{\pi\hbar v_F \rho_0} \right]^{\frac{1}{2-K}}, \quad (10)$$

with ξ_+ a K -dependent constant provided in Ref. [32]. The ground-state energy density is given by $\varepsilon_{\text{gs}}^+ = \frac{2-K}{4\hbar v_F} \cot\left(\frac{\pi}{2-K}\right) [\Delta_R^+]^2 + \dots$, where the ellipsis refer to terms that are independent of Δ [32]. Using this, along with $2\rho_0 \langle \cos[2\phi(x)] \rangle = \partial_\Delta \varepsilon_{\text{gs}}$, we arrive at the following steady-state condition from which to determine $\Phi_{2\pi\rho_0}$,

$$\frac{\Delta}{\pi\hbar v_F \rho_0} = -\eta \frac{\pi \xi_+^2}{2} \cot\left(\frac{\pi}{2-K}\right) \left[\frac{\Delta}{\pi\hbar v_F \rho_0} \right]^{\frac{K}{2-K}}. \quad (11)$$

This has a solution only for $K < 1$. Rearranging, we find that the self-consistent photon field is

$$\langle \Phi(x) \rangle = -\frac{2\pi\hbar v_F \rho_0}{g} \zeta_+ \eta^{\frac{2-K}{2-2K}} \cos(2\pi\rho_0 x), \quad (12)$$

where the constant ζ_+ is given in Ref. [32]. The amplitude of the photon field now displays a power law rather than the exponential dependence on the dimensionless coupling manifest in the TG limit. The free limit $K \rightarrow 1$ cannot be recovered from the above expression and needs to be treated separately as in the previous section. This highlights the strongly correlated nature of the interacting system. The photon field oscillates with wavevector $2\pi\rho_0$, corresponding to $2K$

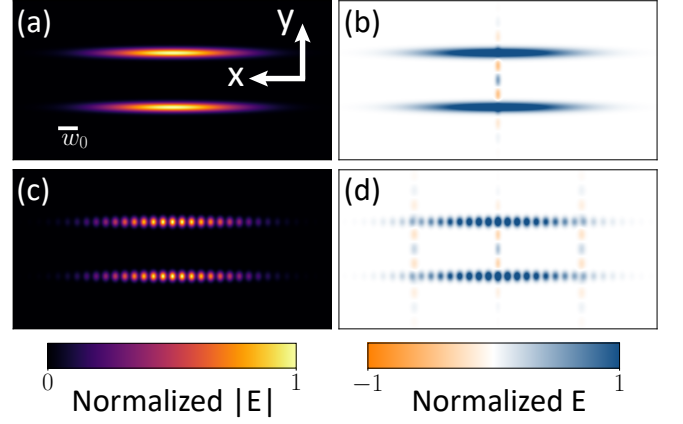


FIG. 2. Simulated intracavity field amplitude at the atoms (a) below and (c) above the transition showing a density wave of wavevector $k = \pi/(0.6w_0)$. Panels (b) and (d) show cavity emission (b) below and (d) above the transition. Emission from a confocal cavity contains both an image of the atomic density (horizontal blue pattern) and its Fourier transform (vertical blue and orange patterns). These can be measured by holographic reconstruction of a spatial heterodyne image [6, 13]. The scale bar in panel (a) indicates the Gaussian waist w_0 of the cavity.

times the Fermi wavevector. The single particle excitation spectrum of the interacting system is given by $\epsilon_n = \Delta_R^+ \cosh \left[\frac{1}{2-K} \operatorname{arcsinh} \left(\frac{\hbar v_F k_n}{\Delta} \right) \right]$ [32]. Thus, the mass gap is $2\Delta_R^+ = 2\pi\hbar v_F \rho_0 \xi_+ [\zeta_+ \eta]^{\frac{1}{2-2K}}$ and the system is insulating.

For $g\Phi_{2\pi\rho_0} > 0$, the model maps to the massive Thirring model, but with a negative mass parameter. As explained in Ref. [32], this change in sign of the mass term results in the spectrum of the model being inverted, i.e., the ground state becomes the highest excited state [32]. Spectral inversion also occurs when changing the sign of the interactions—i.e., taking $K \rightarrow 1/K$. Combining these two facts, we find that for $g\Phi_{2\pi\rho_0} > 0$ and $K > 1$, the renormalized mass gap and self-consistent photon field are

$$\frac{\Delta_R^-}{\pi\hbar v_F \rho_0} = \xi_- \left[\frac{\Delta}{\pi\hbar v_F \rho_0} \right]^{\frac{K}{2K-1}}, \quad (13)$$

$$\langle \Phi(x) \rangle = \frac{2\pi\hbar v_F \rho_0}{g} \zeta_- \eta^{\frac{2K-1}{2K-2}} \cos(2\pi\rho_0 x), \quad (14)$$

where ξ_- , ζ_- are related to ξ_+ , ζ_+ by $K \rightarrow 1/K$.

Experimental signatures — One may image the atomic density profile by using the spatial resolving power of the degenerate cavity. This provides a direct signature of the Peierls instability as a density wave. Figure 2 plots the simulated steady-state intracavity field below and above the Peierls transition, calculated using results from Ref. [12]. The spatial modulation of the light amplitude from the atomic image is a signature of the Peierls transition; a mirror image appears at $-y_t$. The geometry of

the confocal cavity conveniently provides the simultaneous emission of both the atomic density image (long thin tubes) and its Fourier transform (vertical stripes) [12]. Thus, a density modulation of wavevector $2k$ results in the emission of Bragg peaks manifest as vertical stripes. These are positioned a distance $d = \pm kw_0^2$ along \hat{x} from the 0th-order peak at the cavity center (itself just the Fourier transform of the \hat{y} -displaced atom image).

The power-law scaling between the oscillation amplitude of the detected light field and the parameter η depends critically on the atom interactions; see Eq. (12). The Luttinger parameter K can thus be experimentally measured through the dependence of this exponent on η . This parameter can be tuned through its dependence on the pump intensity via $\eta \propto g^2 \propto \Omega^2$, or by the effective photon frequency ω controlled by pump-cavity detuning.

Probing the system by stimulating a particular photon mode realizes cavity-enhanced Bragg spectroscopy [44]. In a degenerate cavity, the probe field profile can be tailored with holographic beam shaping to have a particular intensity modulation wavevector. Thus, dynamic susceptibility can be measured as a function of k and excitation energy ω by also tuning the relative frequency between the probe and pump beam. The response of the system manifests as an increase in photon population, which allows the gap Δ_R^\pm to be measured.

In conclusion, we have shown that multimode confocal cavities can be used to realize the Peierls transition for both Bose and Fermi gases. Away from the simple limits of noninteracting fermions or TG bosons, the scaling of the detected light field with pump strength can be used to measure the Luttinger parameter. Looking beyond Peierls transitions, the compliant, phonon-supporting optical lattices inherent in multimode cavity QED make accessible a wider variety of many-body physics explorable in the context of quantum simulation.

This work was supported by the NSF DMR-1613029 (V.G.), US-ARO contracts W911NF1310172 (V.G.) and W911NF1910262 (B.L.), DARPA DRINQS program (C.R. & V.G.), DOE-BES award DESC0001911 (V.G.), and the Simons Foundation (V.G.). Y.G. acknowledges funding from the Stanford Q-FARM Graduate Student Fellowship.

[1] I. Bloch, J. Dalibard, and W. Zwerger, Many-body physics with ultracold gases, *Rev. Mod. Phys.* **80**, 885 (2008).
 [2] S. Gopalakrishnan, B. Lev, and P. Goldbart, Emergent crystallinity and frustration with Bose-Einstein condensates in multimode cavities, *Nat. Phys.* **5**, 845 (2009).
 [3] S. Gopalakrishnan, B. L. Lev, and P. M. Goldbart, Atom-light crystallization of Bose-Einstein condensates in multimode cavities: Nonequilibrium classical and quantum phase transitions, emergent lattices, supersolidity, and

frustration, *Phys. Rev. A* **82**, 043612 (2010).
 [4] P. Domokos and H. Ritsch, Collective cooling and self-organization of atoms in a cavity, *Phys. Rev. Lett.* **89**, 253003 (2002).
 [5] J. Lonard, A. Morales, P. Zupancic, T. Esslinger, and T. Donner, Supersolid formation in a quantum gas breaking a continuous translational symmetry, *Nature* **543**, 87-90 (2017).
 [6] R. M. Kroeze, Y. Guo, V. D. Vaidya, J. Keeling, and B. L. Lev, Spinor Self-Ordering of a Quantum Gas in a Cavity, *Phys. Rev. Lett.* **121**, 163601 (2018).
 [7] J. Klinder, H. Keßler, M. R. Bakhtiari, M. Thorwart, and A. Hemmerich, Observation of a Superradiant Mott Insulator in the Dicke-Hubbard Model, *Phys. Rev. Lett.* **115**, 230403 (2015).
 [8] R. Landig, L. Hruby, N. Dogra, M. Landini, R. Mottl, T. Donner, and T. Esslinger, Quantum phases from competing short- and long-range interactions in an optical lattice, *Nature* **532**, 476 (2016).
 [9] R. M. Kroeze, Y. Guo, and B. L. Lev, Dynamical Spin-Orbit Coupling of a Quantum Gas, *Phys. Rev. Lett.* **123**, 160404 (2019).
 [10] A. Kollr, A. Papageorge, K. Baumann, M. Armen, and B. Lev, An adjustable-length cavity and Bose-Einstein condensate apparatus for multimode cavity QED, *New J. Phys.* **17** (2014).
 [11] V. D. Vaidya, Y. Guo, R. M. Kroeze, K. E. Ballantine, A. J. Kollár, J. Keeling, and B. L. Lev, Tunable-Range, Photon-Mediated Atomic Interactions in Multimode Cavity QED, *Phys. Rev. X* **8**, 011002 (2018).
 [12] Y. Guo, V. D. Vaidya, R. M. Kroeze, R. A. Lunney, B. L. Lev, and J. Keeling, Emergent and broken symmetries of atomic self-organization arising from Gouy phase shifts in multimode cavity QED, *Phys. Rev. A* **99**, 053818 (2019).
 [13] Y. Guo, R. M. Kroeze, V. D. Vaidya, J. Keeling, and B. L. Lev, Sign-changing photon-mediated atom interactions in multimode cavity quantum electrodynamics, *Phys. Rev. Lett.* **122**, 193601 (2019).
 [14] K. E. Ballantine, B. L. Lev, and J. Keeling, Meissner-like Effect for a Synthetic Gauge Field in Multimode Cavity QED, *Phys. Rev. Lett.* **118**, 045302 (2017).
 [15] C. Chin, R. Grimm, P. Julienne, and E. Tiesinga, Feshbach resonances in ultracold gases, *Rev. Mod. Phys.* **82**, 1225 (2010).
 [16] E. Haller, M. J. Mark, R. Hart, J. G. Danzl, L. Reichsöllner, V. Melezhik, P. Schmelcher, and H.-C. Nägerl, Confinement-Induced Resonances in Low-Dimensional Quantum Systems, *Phys. Rev. Lett.* **104**, 153203 (2010).
 [17] B. Paredes, A. Widera, V. Murg, O. Mandel, S. Fölling, I. Cirac, G. Shlyapnikov, T. Haensch, and I. Bloch, Tonks-Girardeau gas of ultracold atoms in an optical lattice, *Nature* **429**, 277 (2004).
 [18] T. Kinoshita, T. Wenger, and D. Weiss, Observation of a one-dimensional Tonks-Girardeau gas, *Science* **305**, 1125 (2004).
 [19] E. Haller, M. Gustavsson, M. J. Mark, J. G. Danzl, R. Hart, G. Pupillo, and H.-C. Nägerl, Realization of an Excited, Strongly Correlated Quantum Gas Phase, *Science* **325**, 1224 (2009).
 [20] T. Giamarchi, *Quantum Physics in One Dimension*, International Series of Monographs on Physics (Clarendon Press, 2003).
 [21] A. Gogolin, A. Nersisyan, and A. Tsvelik, *Bosonization and Strongly Correlated Systems* (Cambridge University

- Press, 2004).
- [22] A. M. Tsvelik, *Quantum Field Theory in Condensed Matter Physics*, 2nd ed. (Cambridge University Press, 2003).
 - [23] R. Peierls, *Quantum Theory of Solids*, International Series of Monographs on Physics (Clarendon Press, 1996).
 - [24] W. P. Su, J. R. Schrieffer, and A. J. Heeger, Solitons in polyacetylene, *Phys. Rev. Lett.* **42**, 1698 (1979).
 - [25] L. Tonks, The complete equation of state of one, two and three-dimensional gases of hard elastic spheres, *Phys. Rev.* **50**, 955 (1936).
 - [26] M. Girardeau, Relationship between Systems of Impenetrable Bosons and Fermions in One Dimension, *J. Math. Phys.* **1**, 516 (1960).
 - [27] J. Keeling, M. J. Bhaseen, and B. D. Simons, Fermionic superradiance in a transversely pumped optical cavity, *Phys. Rev. Lett.* **112**, 143002 (2014).
 - [28] F. Piazza and P. Strack, Umklapp Superradiance with a Collisionless Quantum Degenerate Fermi Gas, *Phys. Rev. Lett.* **112**, 143003 (2014).
 - [29] Y. Chen, Z. Yu, and H. Zhai, Superradiance of Degenerate Fermi Gases in a Cavity, *Phys. Rev. Lett.* **112**, 143004 (2014).
 - [30] A. E. Siegman, *Lasers* (University Science Books, 1986).
 - [31] K. Baumann, C. Guerlin, F. Brennecke, and T. Esslinger, The Dicke Quantum Phase Transition with a Superfluid Gas in an Optical Cavity, *Nature* **464**, 1301 (2010).
 - [32] See Supplemental Material at for information on the origin of the effective Hamiltonian, details of the calculation of the Ground state and solution of the self consistency equation, and discussion of realistic experimental parameters.
 - [33] Extending the array along \hat{y} is possible, but does not change the physics.
 - [34] P. Kirton, M. M. Roses, J. Keeling, and E. G. Dalla Torre, Introduction to the Dicke model: From equilibrium to nonequilibrium, and vice versa, *Adv. Quantum Technol.* **2**, 1800043 (2019).
 - [35] See Ref. [12] for near-degenerate case where the interaction becomes finite in range; Peierls physics remains the same as long as the interaction range is less than the intertube spacing.
 - [36] F. Damanet, A. J. Daley, and J. Keeling, Atom-only descriptions of the driven-dissipative Dicke model, *Phys. Rev. A* **99**, 033845 (2019).
 - [37] S. Coleman, Quantum sine-Gordon equation as the massive Thirring model, *Phys. Rev. D* **11**, 2088 (1975).
 - [38] F. Haldane, Effective harmonic-fluid approach to low-energy properties of one-dimensional quantum fluids, *Phys. Rev. Lett.* **47**, 1840 (1981).
 - [39] M. A. Cazalilla, Bosonizing one-dimensional cold atomic gases, *J. Phys. B* **37**, S1 (2004).
 - [40] M. A. Cazalilla, R. Citro, T. Giamarchi, E. Orignac, and M. Rigol, One dimensional bosons: From condensed matter systems to ultracold gases, *Rev. Mod. Phys.* **83**, 1405 (2011).
 - [41] A. Luther and V. J. Emery, Backward scattering in the one-dimensional electron gas, *Phys. Rev. Lett.* **33**, 589 (1974).
 - [42] H. Bergknoff and H. B. Thacker, Structure and solution of the massive Thirring model, *Phys. Rev. D* **19**, 3666 (1979).
 - [43] A. B. Zamolodchikov and A. B. Zamolodchikov, Factorized S-Matrices in Two Dimensions as the Exact Solutions of Certain Relativistic Quantum Field Theory Models, *Ann. Phys.* **120**, 253 (1979).
 - [44] R. Mottl, F. Brennecke, K. Baumann, R. Landig, T. Donner, and T. Esslinger, Roton-type mode softening in a quantum gas with cavity-mediated long-range interactions, *Science* **336**, 1570 (2012).
 - [45] H. Ritsch, P. Domokos, F. Brennecke, and T. Esslinger, Cold atoms in cavity-generated dynamical optical potentials, *Rev. Mod. Phys.* **85**, 553 (2013).
 - [46] M. Takahashi, *Thermodynamics of One-Dimensional Solvable Models* (Cambridge University Press, 1999).
 - [47] H. B. Thacker, Exact Integrability in Quantum Field Theory and Statistical Systems, *Rev. Mod. Phys.* **53**, 253 (1981).

SUPPLEMENTAL MATERIAL

ORIGIN OF THE EFFECTIVE HAMILTONIAN

In this section, we discuss the origin of the matter-light interaction in Eq. (1), starting from a more general description of coupling between atoms and photons in a multimode cavity. In general, the interaction between light and matter can be written as $H_{\text{atom,cavity}} = \int d^3\mathbf{r} \Psi^{3D,\dagger}(\mathbf{r}) \Psi^{3D}(\mathbf{r}) |\beta(\mathbf{r})|^2 / \Delta_a$, where Δ_a is the atom-pump detuning, and we have written a rescaled total light field β , including the bare matter-light coupling constant. This coupling corresponds to the standard light shift of atoms by an optical field [12, 45]. The total light field has two parts; that from the transverse pump along \hat{y} , and that from the cavity along \hat{z} :

$$\beta(\mathbf{r}) = \Omega \cos(k_r y) + g_0 \sum_{\alpha,\nu} \hat{a}_{\alpha,\nu} \Xi_\nu(x, y) \cos \left[k_r \left(z + \frac{x^2 + y^2}{R(z)} \right) - \theta_{\alpha,\nu}(z) \right], \quad (\text{S1})$$

where the Gouy phase is given by $\theta_{\alpha,\nu}(z) = \psi(z) + n_\nu[\pi/4 + \psi(z)] - \xi_{\alpha,\nu}$, with $\psi(z) = \text{atan}(z/z_R)$, the radius of curvature $R(z) = z + z_R^2/z$, and z_R the Rayleigh range. This is $z_R = L/2$ for a confocal cavity. The transverse mode functions $\Xi_\nu(x)$ are Gauss-Hermite functions of order (l_ν, m_ν) in the x and y directions, respectively.

As discussed in the main text, we consider atoms trapped in tubes along \hat{x} , so that we can write $\Psi^{(3D)}(\mathbf{r}) = \sum_t \Psi_t(x) \psi_0(y - y_t, z - z_t)$, with $\psi_0(y, z)$ describing the trapped atomic Gaussian profile of a single tube in the yz plane and y_t, z_t indicating the center position of each tube. We assume the trapping profile is narrow compared to the wavelength of the pump and cavity light, and that, as noted in the main text, the tubes trap atoms at the maxima of both fields, where $k_r \lambda_T / 2\pi$ is an integer. The light shift $\propto |\beta(\mathbf{r})|^2$ gives, in general, three types of terms: pump-only, cavity-only, and cross pump-cavity terms. The pump-only terms induce a constant energy shift and so may be ignored. We will consider the case where the bare coupling g_0 is much smaller than Ω , so that the cavity-only term is negligible. We can therefore focus on the cross pump-cavity term. Restricting to points near the cavity center, we find this has the form:

$$H_{\text{atom,cavity}} = \frac{\Omega g_0}{\Delta_a} \int dx \sum_t \Psi_t^\dagger(x) \Psi_t(x) \sum_{\alpha,\nu} (\hat{a}_{\alpha,\nu} + \hat{a}_{\alpha,\nu}^\dagger) \tilde{\Xi}_\nu(x, y_t) \cos[-\theta_{\alpha,\nu}(0)]. \quad (\text{S2})$$

This can be rewritten directly in the form given by Eq. (1). In writing this we have introduced the function:

$$\tilde{\Xi}_\nu(x, y_t) = \int dy \Xi_\nu(x, y) |\psi_0(y - y_t)|^2, \quad (\text{S3})$$

convolving the transverse mode functions with the trapped wavefunction. This is important to regularise the singularity of the cavity-mediated interaction at equal positions. Specifically, when considering the sum over modes appearing in the main text we find:

$$\sum_\nu \tilde{\Xi}_\nu(x, y_t) \tilde{\Xi}_\nu(x', y_{t'}) = \int dy |\psi_0(y - y_t)|^2 \int dy' |\psi_0(y' - y_{t'})|^2 \sum_\nu \Xi_\nu(x, y) \Xi_\nu(x', y') \quad (\text{S4})$$

$$= \int dy |\psi_0(y - y_t)|^2 \int dy' |\psi_0(y' - y_{t'})|^2 \frac{w_0^2}{2} [\delta(x - x') \delta(y - y') + \delta(x + x') \delta(y + y')] \quad (\text{S5})$$

where w_0 is the beam waist. If we assume all tubes are in the upper half plane, then we need only consider the term involving $\delta(y - y')$. Assuming a Gaussian profile $|\psi_0(y)|^2 = \exp(-y^2/2\sigma_T^2)/\sqrt{2\pi\sigma_T^2}$ with tube width σ_T one finds the above expression reduces to: $\frac{w_0^2}{2} \delta(x - x') \delta_{t,t'}^Y / (\sqrt{4\pi}\sigma_T)$ where $\delta_{t,t'}^Y$ restricts to tubes at the same position y_t . In the main text, for simplicity, we assume only a single tube position $y_t = y_0$, simplifying this. For this reason, in the main text we wrote $\tilde{\Xi}_\nu(x)$ suppressing the dependence on the (constant) coordinate y_0 .

GROUND-STATE ENERGY OF THE MODEL

We now derive the ground-state energy density for the Sine-Gordon model with both positive and negative mass parameters. To achieve this, we work in the fermionic representation of the Sine-Gordon model, also known as the

massive Thirring model [20, 21, 37]. Using the right and left moving fermion operators $\psi_{\pm}^{\dagger}(x) = \sqrt{\rho_0} e^{\mp i\phi(x) - i\theta(x)}$, the Hamiltonians are given by

$$H_{\text{mtm}}^{\pm} = \int dx \left\{ i\hbar v_F \left[\psi_{-}^{\dagger} \partial_x \psi_{-} - \psi_{+}^{\dagger} \partial_x \psi_{+} \right] \pm \Delta \left[\psi_{+}^{\dagger} \psi_{-} + \psi_{-}^{\dagger} \psi_{+} \right] + 4g_c \psi_{+}^{\dagger} \psi_{-}^{\dagger} \psi_{-} \psi_{+} \right\}, \quad (\text{S6})$$

where the mass parameter is $\Delta = |g\Phi_{2\pi\rho_0}|$ and g_c is the fermionic interaction strength, which is related to the Luttinger parameter K in a way specified below. Therefore, H_{mtm}^{+} corresponds to $\Phi_{2\pi\rho_0} < 0$ and H_{mtm}^{-} corresponds to $\Phi_{2\pi\rho_0} > 0$. For $g_c = 0$, we have the low-energy description of the TG gas from which we derive the Dirac equation used in the main text in Eqs. (6),(7).

The Hamiltonian with either positive or negative mass may be solved exactly via Bethe ansatz and the many-body eigenstates determined explicitly [42]. We introduce the operators $\Lambda^{\dagger}(\theta, x) = e^{\theta/2} \psi_{+}^{\dagger}(x) + e^{-\theta/2} \psi_{-}^{\dagger}(x)$, which in the TG limit are merely the Bogoliubov quasiparticle creation operators for a particle with rapidity θ , or equivalently, momentum $\hbar k = \Delta \sinh(\theta)/v_F$. In terms of these, the N -body wavefunctions of both H_{mtm}^{+} and H_{mtm}^{-} may be written as

$$\int d^N x \prod_{i < j} e^{i\chi(\theta_i - \theta_j) \text{sgn}(x_i - x_j)/2} \prod_{j=1}^N e^{i\Delta \sinh(\theta_j) x_j / \hbar v_F} \Lambda^{\dagger}(\theta_j, x_j) |0\rangle, \quad (\text{S7})$$

where $|0\rangle$ is the vacuum state containing no particles and $\chi(\theta_i - \theta_j)$ is the two particle phase shift [42]

$$e^{i\chi(\theta_i - \theta_j)} = \frac{\sinh[(\theta_i - \theta_j)/2 - i\gamma]}{\sinh[(\theta_i - \theta_j)/2 + i\gamma]}, \quad (\text{S8})$$

$$\gamma = \pi/2 + \arctan(g_c). \quad (\text{S9})$$

The two models share a set of common eigenstates, however the change in sign of the mass results in a change in the eigenvalues of these states that are $E = \pm \sum_{j=1}^N \Delta \cosh(\theta_j)$, with the plus sign for H_{mtm}^{+} and the minus sign for H_{mtm}^{-} . The ground state consists of all the negative energy particles being filled from some cutoff up to zero energy. Therefore, the ground state of H_{mtm}^{+} consists of particles whose rapidities have an imaginary part, $\theta_j = \theta_j^{+} + i\pi$, while for H_{mtm}^{-} the rapidities are purely real, $\theta_j = \theta_j^{-}$. In effect, the two models are related by inverting the spectrum; i.e., the ground state of one model is the highest excited state of the other.

The rapidity parameters θ_j^{\pm} are not free, but instead are coupled together via the Bethe ansatz equations. These are given by [42]

$$e^{\mp i\Delta \sinh(\theta_j^{\pm})L/\hbar v_F} = \prod_{k \neq j} \frac{\sinh[(\theta_j^{\pm} - \theta_k^{\pm})/2 - i\gamma]}{\sinh[(\theta_j^{\pm} - \theta_k^{\pm})/2 + i\gamma]} \quad (\text{S10})$$

and are derived by imposing periodic boundary condition on the wavefunction in Eq. (S7). We may bring the Bethe equations above into a common form by introducing γ^{\pm} with $\gamma^{+} = \gamma$ and $\gamma^{-} = \pi - \gamma^{+}$, which in terms of the interaction strength are $\gamma^{\pm} = \pi/2 \pm \arctan(g_c/v_F)$. This shows that the ground state of H_{mtm}^{\pm} is described by the Bethe equations

$$e^{-i\Delta \sinh(\theta_j^{\pm})L/\hbar v_F} = \prod_{k \neq j} \frac{\sinh[(\theta_j^{\pm} - \theta_k^{\pm})/2 - i\gamma^{\pm}]}{\sinh[(\theta_j^{\pm} - \theta_k^{\pm})/2 + i\gamma^{\pm}]} \quad (\text{S11})$$

and has energy $E_{\text{gs}}^{\pm} = -\sum_{j=1}^N \Delta \cosh(\theta_j^{\pm})$.

In the thermodynamic limit $N, L \rightarrow \infty$, the rapidities can be described by a distribution denoted by $\rho_{\pm}(\theta)$ such that the sum over rapidities is replaced by $\sum_{j=1}^N \rightarrow L \int d\theta \rho_{\pm}(\theta)$. This can subsequently be used to obtain the ground-state energy density $\varepsilon_{\text{gs}}^{\pm} = -\int d\theta \rho_{\pm}(\theta) \Delta \cosh(\theta)$. Taking the logarithm of Eq. (S10) and the thermodynamic limit using standard Bethe ansatz techniques (see, e.g., [46, 47]), we arrive at the integral equation for the rapidity distribution:

$$\frac{\Delta}{2\pi\hbar v_F} \cosh \theta = \rho_{\pm}(\theta) + \int d\nu f_{\pm}(\theta - \nu) \rho_{\pm}(\nu), \quad (\text{S12})$$

$$f_{\pm}(x) = \frac{1}{2\pi} \frac{\sin(2\gamma^{\pm})}{\cosh(x) - \cos(2\gamma^{\pm})}. \quad (\text{S13})$$

The above integrals need to be regulated in some fashion to solve the integral equation. In the TG case, which is equivalent to the BCS and SSH models, a momentum cutoff of $\pi\rho_0$ is imposed, and so we shall also employ the

same strategy in the interacting case. We introduce a rapidity cutoff, \mathcal{K} , which is determined via $\rho_0 = \int_{-\mathcal{K}}^{\mathcal{K}} d\theta \rho_{\pm}(\theta)$. Following the procedure in [47], we find that

$$\rho_{\pm}(\theta) = \frac{\Delta_{\text{R}}^{\pm}}{2\pi\hbar v_F} \cosh \left[\frac{\pi}{2\gamma^{\pm}} \theta \right], \quad (\text{S14})$$

where Δ_{R}^{\pm} is the renormalized mass gap of the interacting model. It is related to Δ via

$$\frac{\Delta_{\text{R}}^{\pm}}{\pi\hbar v_F \rho_0} = \xi_{\pm} \left[\frac{\Delta}{\pi\hbar v_F \rho_0} \right]^{\pi/2\gamma^{\pm}}, \quad (\text{S15})$$

$$\xi_{\pm} = \frac{\pi}{\gamma^{\pm}} \left[\frac{\tan \left(\frac{\pi^2}{2\gamma^{\pm}} \right)}{\pi^2/\gamma^{\pm} - 2\pi} \right]^{\pi/2\gamma^{\pm}}. \quad (\text{S16})$$

From this, we can determine the ground-state energy density in the thermodynamic limit to be

$$\varepsilon_{\text{gs}}^{\pm} = \frac{\hbar v_F}{2} (\pi \rho_0)^2 \left[\frac{2\gamma^{\pm} - \pi}{\pi^2/\gamma^{\pm} + 2\pi} \right] \cot \left(\frac{\pi^2}{2\gamma^{\pm}} \right) + \frac{\gamma^{\pm} [\Delta_{\text{R}}^{\pm}]^2}{2\pi\hbar v_F} \cot \left(\frac{\pi^2}{2\gamma^{\pm}} \right). \quad (\text{S17})$$

Note that this expression is negative only for $\gamma^{\pm} > \pi/3$ and so is actually only the ground state of the model within the regime $\gamma^{\pm} > \pi/3$, excluding the point $\gamma^{\pm} = \pi/2$. That point corresponds to the TG case and needs to be separately considered.

In order to relate these expressions back to the bosonized version of the model, Eq. (5), we need to express γ in terms the Luttinger parameter K . For the positive mass model the relation is known to be $2\gamma^+/\pi = 2 - K$ [42, 43]. To find a similar relationship for the negative mass model, we use the fact that the two are related by $g_c \rightarrow -g_c$, which within bosonization is equivalent to $K \rightarrow 1/K$ [20, 21], and therefore $2\gamma^-/\pi = 2 - 1/K$.

The basic excitations of H_{mtm}^{\pm} consist of adding holes or particles on top of the ground states described above. The addition of a hole to the ground state distribution at θ^h leads to a shift $\rho_{\pm}(\theta) \rightarrow \rho_{\pm}(\theta) + \delta\rho_{\pm}(\theta)$ due to the interactions in the model. The shift is a solution to the integral equation,

$$-\delta(\theta - \theta^h) = \delta\rho_{\pm}(\theta) + \int d\nu f_{\pm}(\theta - \nu) \rho_{\pm}(\nu), \quad (\text{S18})$$

which can be solved via Fourier transform. The change in energy due to the presence of the hole provides us with the single-particle excitation spectrum, i.e., the energy of the hole $\varepsilon^h(\theta^h)$:

$$\varepsilon(\theta^h) = -\Delta \int d\theta \cosh(\theta) \delta\rho_{\pm}(\theta) = 2\pi\rho_{\pm}(\theta^h) \quad (\text{S19})$$

$$= \Delta_{\text{R}}^{\pm} \cosh \left[\frac{\pi}{2\gamma^{\pm}} \theta \right]. \quad (\text{S20})$$

We can translate this into the more familiar language of particle momenta using $\Delta \sinh(\theta) = \hbar v_F k$:

$$\varepsilon^h(k) = \Delta_{\text{R}}^{\pm} \cosh \left[\frac{\pi}{2\gamma^{\pm}} \text{arcsinh} \left(\frac{\hbar v_F k}{\Delta} \right) \right]. \quad (\text{S21})$$

In the TG limit, this reproduces $\varepsilon = \sqrt{(\hbar v_F k)^2 + \Delta^2}$ and shows that the gap is given by Δ_{R}^{\pm} .

The excitations of the full system, both atom and cavity, consist of an atomic excitation with momentum $\hbar k$ and an associated shift of the photon field $\Delta'_k = \Delta + \delta\Delta_k$ such that

$$\Delta'_k = -\pi\hbar v_F \eta \frac{d}{d\Delta'} [\varepsilon_{\text{gs}}(\Delta'_k) + \varepsilon_k(\Delta'_k)/L], \quad (\text{S22})$$

where $\varepsilon_k(\Delta'_k)$ is the expression given in (S21), but evaluated at Δ'_k . From this, we have that to leading order, the shift in the photon field is $\delta\Delta_k = -\pi\hbar v_F \eta (\frac{d\varepsilon_k(\Delta)}{d\Delta})/L$. The total shift in energy caused by this excitation is then given by

$$\delta E_k = L\delta\Delta_k \frac{d\varepsilon_{\text{gs}}(\Delta)}{d\Delta} + \frac{L}{\pi\hbar v_F \eta} \delta\Delta_k \Delta + \varepsilon_k(\Delta), \quad (\text{S23})$$

where the first term in the first line comes from the shift in the ground-state energy density due to the change in Δ , the second is the change in the photon energy and the last is the energy of the atomic excitation which is positive. Upon using the self-consistency condition, we find the first and second terms cancel and $\delta E_k = \varepsilon_k(\Delta)$.

SOLUTION OF THE SELF CONSISTENCY EQUATION

The steady-state/self-consistency condition in the interacting case is

$$\Delta = -\pi\hbar v_F \eta \frac{d\varepsilon_{gs}^{\pm}}{d\Delta}. \quad (\text{S24})$$

Using the expression from the last section, we have that

$$\frac{d\Delta_R^{\pm}}{d\Delta} = \frac{\pi\xi_{\pm}}{2\gamma^{\pm}} \left[\frac{\Delta}{\pi\hbar v_F \rho_0} \right]^{\pi/2\gamma^{\pm}-1}. \quad (\text{S25})$$

Inserting this into Eq. (S24), we have

$$\frac{\Delta}{\pi\hbar v_F \rho_0} = -\eta \cot\left(\frac{\pi^2}{2\gamma^{\pm}}\right) \frac{\pi\xi_{\pm}^2}{2} \left[\frac{\Delta}{\pi\hbar v_F \rho_0} \right]^{\pi/\gamma^{\pm}-1}. \quad (\text{S26})$$

The left hand side of this equation is positive by definition whereas the right hand side is positive only for $\gamma^{\pm} > \pi/2$: A solution is only possible within this regime. Restricting to these cases, $K < 1$ for H_{mtm}^{+} or $K > 1$ for H_{mtm}^{-} , and rearranging, we find

$$\frac{\Delta}{\pi\hbar v_F \rho_0} = \zeta_{\pm} \eta^{\gamma^{\pm}/(2\gamma^{\pm}-\pi)}, \quad (\text{S27})$$

where the proportionality constant is

$$\zeta_{\pm} = \left[\frac{\pi\xi_{\pm}^2}{2} \left| \cot\left(\frac{\pi^2}{2\gamma^{\pm}}\right) \right| \right]^{\gamma^{\pm}/(2\gamma^{\pm}-\pi)} \quad (\text{S28})$$

$$= \frac{\pi}{\gamma^{\pm}} \left[\frac{\pi}{4\gamma^{\pm} - 2\pi} \right]^{\gamma^{\pm}/(2\gamma^{\pm}-\pi)} \sqrt{\frac{\tan\left(\frac{\pi^2}{2\gamma^{\pm}}\right)}{2\gamma^{\pm} - \pi}}. \quad (\text{S29})$$

We can express the renormalized mass parameters in terms of this result:

$$\frac{\Delta_R^{\pm}}{\pi\hbar v_F \rho_0} = \xi_{\pm} \zeta_{\pm}^{\pi/2\gamma^{\pm}} \eta^{\pi/(4\gamma^{\pm}-2\pi)}. \quad (\text{S30})$$

REALISTIC EXPERIMENTAL PARAMETERS

In this section, we discuss the experimental feasibility of observing the Peierls transition in a 1D system realized with bosonic ^{87}Rb atoms. Previous experiments have achieved the Tonks-Girardeau limit by trapping ^{87}Rb in a 2D optical lattice with sufficient lattice depth [18]. To stay within the validity of the low-energy description and maintain sufficient photon population, we require $\eta \lesssim 1$ in Eq. (9). In the experiment, the 1D tubes are tightly confined in the transverse direction, with typical excitation energy of ~ 100 kHz, corresponding to a harmonic oscillator length scale of ~ 30 nm. This is far below the wavelength of the cavity light. As such, the parameter σ_T in the expression of η is determined by the minimum spot size supported by the multimode cavity. In previous work, the smallest spot size measured, ~ 1 μm , was in fact limited by the atomic cloud size. We use this estimate as a conservative upper bound. Using cavity QED parameters from Ref. [11], we find (with a pump and cavity -100 GHz detuned from the D_2 -line of ^{87}Rb) that $\eta \approx 0.8$ is achieved with 100 tubes, $0.5/\mu\text{m}$ atomic linear density, and a pump Rabi frequency of ~ 50 MHz at -20 MHz pump-cavity detuning. These conditions are realizable with existing technology. The typical temperature of the gas is around 1–10 nK, which is smaller than the mass gap $\Delta \approx k_B \cdot 15$ nK. The spontaneous emission rate at such pump power and atomic detuning is ~ 2 Hz, leaving ample time for observing the instability.